
Research on application of optimization installation position for spur gear in gear rack drilling rig transmission unit

Wang Jiangang¹ Feng Ding^{2*} Shi Lei³ Sun Qiaolei⁴ Miao Enming⁵

1 Ph.D. student. Institute for Hubei Engineering Research Center for Oil & Gas Drilling and Completion Tools. Dept. of Mechanical Engineering, Yangtze University, Jingzhou, Hubei, 434023, China. Email: 371152725@163.com.

2 Professor. Institute for Hubei Engineering Research Center for Oil & Gas Drilling and Completion Tools. Dept. of Mechanical Engineering, Yangtze University, Jingzhou, Hubei, 434023, China. Email: fengd0861@163.com, Tel: +86 13607219921. * Corresponding author.

3 Associate professor. student. Institute for Hubei Engineering Research Center for Oil & Gas Drilling and Completion Tools. Dept. of Mechanical Engineering, Yangtze University, Jingzhou, Hubei, 434023, China. Email: shilei0909@163.com.

4 Associate professor. Institute for Hubei Engineering Research Center for Oil & Gas Drilling and Completion Tools. Dept. of Mechanical Engineering, Yangtze University, Jingzhou, Hubei, 434023, China. Email: 649647220@qq.com.

5. Professor. College of Mechanical Engineering, Chongqing University of Technology, Chongqing 401135, China. Email: 2695522528@qq.com.

Abstract: The gear and rack transmission unit is a crucial load transmission device in the Gear Rack Drilling Rig (GRDR). Vibration induced by stiffness excitation during meshing between the gear and rack is a significant factor that affects the transmission performance. This paper focuses on the transmission unit of the GRDR and proposes a gear position design method based on time-varying meshing stiffness. A time-varying mesh stiffness model is established, considering tooth profile by the slice-iteration method. With the White Shark Optimizer (WSO) global search optimization algorithm, the gear position conditions are explored based on the fluctuation of stiffness. The load-bearing performance and dynamic characteristics of the mechanism are effectively improved. Dynamic analysis is conducted before and after the optimization of the scheme, and the improvements of the gear position optimization to the displacement of the transmission mechanism are verified through the meshing process of the rack and gear. The results show that the proposed optimization design may reduce the fluctuation by 89.64% and the maximum displacement by 9% compared to before. The proposed design method can effectively improve the motion performance, which is significant for optimizing the transmission unit of the GRDR.

Keywords: Gear Rack Drilling Rig, Transmission unit, Rack and Gear, Time-Varying Meshing Stiffness, Optimization.

28 0 Introduction

29 The global oil industry plays a vital role in driving economic development. To enhance the economic
30 efficiency of oil extraction, increasing the efficiency of drilling operations and shortening the drilling cycle
31 is imperative[1]. Traditional drilling rigs apply drilling pressure using the weight of the travel system, which
32 may be insufficient, especially in shallow and horizontal drilling sections, thereby reducing efficiency. The
33 Gear Rack Rig (GRDR), a novel active pressurized drilling rig[2, 3], has been developed to tackle this
34 challenge. The GRDR increases the bit weight during drilling and utilizes a gear and rack mechanism for
35 both bit pressure transmission and drill string lifting. The dynamic performance of the mechanism is a
36 critical factor that affects the structural mechanical response and the safety performance of the drilling rig[4,
37 5, 6]. Therefore, it is imperative to ensure a reasonable design of the transmission unit. Overall, the
38 development of the GRDR represents a promising avenue for improving the efficiency of oil extraction.

39 The GRDR transmission unit has the characteristics of low speed and heavy load. Strength calculation
40 based on statics cannot meet the requirements of the gear and rack vibration. Vibration induced by stiffness
41 is an important factor affecting the dynamic performance and service life of gear-rack transmission unit [7,
42 8]. A large number of scholars have carried out a series of studies. Considering the influence of time-varying
43 meshing stiffness, Zhang[9] established the dynamic model of Epicyclic gear, and an optimal design method
44 based on genetic algorithm was proposed. The results show that the effect of time-varying meshing stiffness
45 on load-sharing performance is obvious. Younes[10] examined how tooth profiles and geometric
46 parameters of gears affect their stiffness. This study utilized the genetic algorithm NSGA-II for multi-
47 objective optimization, focusing on improving transmission efficiency and reducing errors. Offshore
48 platform transmission systems optimize the number of teeth in gear meshes to minimize vibration, shock,

49 and noise during gear rack transmission.[11]. Mounica[12]studied the 7-gear rack lifting system by using
50 finite element method to obtain the optimal fillet radius of gear teeth. On this basis, considering the effect
51 of meshing position on gear stress. Kondaker[13] studied the mechanical response of gear/rack transmission
52 unit and stiffness analysis of gear shaft. However, the stress analysis is only focused on the gear single
53 contact under static load. Gear rack transmission unit is used to lift drill string in land drilling rigs, and the
54 related literature is very limited. Base on the transmission unit of six gears and four racks as the research
55 object, Feng[2]studied the load-carrying capacity of the gear and rack in the meshing process through the
56 finite element method. Lei[14] studied the stability and strength check of the meshing process considering
57 the load. The result shows that the force load of the gear under the asymmetric load is larger than that on
58 the other side. Literature review shows that the work of gear rack transmission unit in GRDR is very limited,
59 especially the research report on reducing stiffness fluctuation through parameter optimization.

60 This study investigates the optimal gear installation positions within the transmission unit of a gear
61 rack drilling rig to enhance stability and reduce vibration and shock during operation. It develops an
62 advanced mesh stiffness model considering specific gear and rack tooth profiles. The impact of gear
63 placement on meshing tooth count is analyzed while ensuring internal collision space constraints are
64 observed. Optimization focuses on minimizing Time-Varying Meshing Stiffness (TVMS) fluctuations using
65 the Whale Shark algorithm. Validation includes integrating a dynamic transmission model with field tests
66 to ensure optimization reliability.

67 1 Problem description

68 The rigid connection between the gear and rack causes more pronounced vibration in the drilling rig
69 compared to the traditional drilling rig with wire ropes. The gear and rack transmission unit is a crucial

70 component of the GRDR and serves as the fundamental equipment for ensuring drilling performance and
71 reliability of the transmission unit. In this paper, the GRDR transmission unit, which features an 8-gear and
72 4-rack back-to-back style transmission, as the primary research object. The gears are designed with a large
73 module, which offers the advantage of high load-carrying capacity. The transmission unit is formed by
74 installing the gear on the box and fixing the rack to the rig derrick, as shown in Figure 1. The transmission
75 unit and Derrick's center of gravity are located in the same plane, providing several technical benefits, such
76 as uniform forces on each gear, reduced friction of the guide wheel during lifting, and more flexibility in
77 gear design size. Influenced by the working conditions, the transmission unit is characterized by low speed
78 and heavy load. Optimization of gear parameters is used in gear design, but the approach lacks advantages
79 in economy. The vibration in the transmission unit is caused by the dynamic excitation resulting from the
80 periodic changes in the gear contact.

81 The transmission unit is a parallel symmetrical distribution of eight gears, which the front gears are
82 used as the research object. The phase difference between the initial gears is considered to be 0° . As shown
83 in Figure 2, the number of gear meshing teeth before optimization varied greatly at different moments,
84 which resulted in the TVMS large fluctuation of TVMS. Installation positions of the gears are optimized to
85 enhance the dynamics. Amplitude of change in the gear mesh tooth number is reduced, which in result
86 reduces the TVMS fluctuation.

87 2 Description of gear mounting position design method

88 The investigation of gear installation position design proceeds through three sequential steps, outlined
89 in Figure 3: establishing the "gear and rack TVMS model," reducing transmission unit TVMS fluctuation,
90 and verifying dynamic performance. Each step aims to achieve specific research objectives. The gear and

91 rack TVMS model is developed by integrating structural parameters of the gear and rack with theories such
92 as Hamiltonian, energy, and Muskhelishvili fillet theories. Optimization of gear installation positions
93 utilizes the white shark optimization algorithm, taking into account its impact on TVMS fluctuation. The
94 reliability of this optimization approach is subsequently validated through dynamic performance
95 calculations and testing.

96 Stiffness is a key factor in determining the vibration displacement correlation function in the dynamic
97 formula, and therefore has a significant impact on the overall dynamic performance of transmission unit.
98 To enhance the stability of the transmission unit, a novel design optimization method is proposed that can
99 effectively accommodate internal collision constraints. In this method the installation position of the gears
100 is optimized by which the fluctuation of the TVMS of the gears is reduced. The phase difference between
101 the gears is modified and the magnitude of variation in the number of meshed teeth at different moments is
102 decreased.

103 2.1 Objective functions and constraints

104 The optimization model for multi-gear TVMS is characterized as a nonlinear programming problem
105 in which the design variables need to be re-selected in each iteration. An objective function for the
106 optimization problem is proposed, which aims to minimize the variance of multi-gear TVMS in a cycle.
107 The objective function is composed of the four gears TVMS and is influenced by the gear installation
108 distance. Specifically, Equation (1) is used to calculate the stiffness fluctuation value during the gear
109 transmission process and optimize the installation distance of the multi-gears system.

$$110 \quad \min f = \delta \left(G_{x_1} + G_{x_2} + G_{x_3} + G_{x_4} \right) \quad (1)$$
$$G_{x_i} = [G_o(x_i:), G_o(1:x_i)]$$

111 Where δ is calculated variance, x_i is relative to the pre-design changes in the location of each gear,

112 G_{x_i} is the gear at the installation distance of the TVMS.

113 When the installation distance of gears is designed, the space constraints of hydraulic motors, reducers,
114 and other devices are considered. To satisfy the practical engineering requirements, the design parameters
115 are set to integer values. The constraint function is presented in Equation (2), where all the above factors
116 are considered and the constraints on the gear mounting position are satisfied.

$$117 \quad \begin{aligned} 0 &\leq x_i \leq 62 \\ x_i &\in z \end{aligned} \quad (2)$$

118 2.2 Time-varying meshing stiffness

119 The TVMS is composed of bending, shear, axial compressive, contact and fillet-foundation. The gear
120 and rack TVMS is calculated as shown in Equation (3):

$$121 \quad K_e = \frac{1}{\frac{1}{K_{a1}} + \frac{1}{K_{b1}} + \frac{1}{K_{s1}} + \frac{1}{K_{f1}} + \frac{1}{K_h} + \frac{1}{K_{a2}} + \frac{1}{K_{b2}} + \frac{1}{K_{s2}} + \frac{1}{K_{f2}}} \quad (3)$$

122 The stiffness of single teeth mesh by calculating axial(k_a) Shear(k_s), bending(k_b), fillet-foundation
123 stiffness(K_f), subscripts 1 and 2 denote gear and rack, respectively.

124 2.2.1 Function of tooth profile

125 The profile of the gear tooth is constituted by the gear tooth structure and the pressure angle, which is
126 influenced by the TVMS by the tooth profile. The tooth profile curve comprises the straight-line and curve
127 types, as depicted in Figure 4. The tooth profile of the research object is composed of straight line and curve.
128 The gear tooth profile curve is composed of involute tooth profile, linear profile, and tooth root arc. The
129 rack consists of straight line and tooth root circular profiles, where the involute tooth profile, root circular
130 tooth profile, and linear tooth profile are represented in Equation (4)-(6), respectively:

131 Involute tooth profile:

$$\left. \begin{aligned} x &= r_i \sin(\pi / 2N - (\text{inv } \alpha_i - \text{inv } \alpha_0)) \\ y &= r_i \cos(\pi / 2N - (\text{inv } \alpha_i - \text{inv } \alpha_0)) \end{aligned} \right\} \quad (4)$$

Where r_i is the distance from the engaging point to the center of the gear; N is the number of teeth;

$\text{inv } \alpha_i$ is the involute Angle on the circle of radius r_i , $\text{inv } \alpha_0$ is the involute Angle of the pitch diameter.

Root circular tooth profile:

$$\left. \begin{aligned} x &= r \times \sin \phi - (a_1 / \sin \gamma + r_\rho) \times \cos(\gamma - \phi) \\ y &= r \times \cos \phi - (a_1 / \sin \gamma + r_\rho) \times \sin(\gamma - \phi) \end{aligned} \right\} \quad (5)$$

Where r is reference radius. r_ρ is the distance between the center of the Fillet and the center line,

a_1 is the radius of the fille.

Straight Line of tooth profile:

$$y = y_L - \tan(\alpha_r)x \quad (6)$$

Where y_L is the distance from the intersection point of meshing line and the root circle to the center,

α_r is the Pressure Angle of rack.

2.22 Function of single tooth stiffness

The property of meshing stiffness is affected by structure and material parameters, such as module,

number of teeth, pressure angle, tooth width, and material, which directly influence the value of meshing

stiffness. The stiffness of a single tooth is determined through the calculation of the bending, shearing, and

axial directions of each tooth, as depicted in Equation (7):

$$\begin{aligned} \frac{1}{k_b} &= \int_0^d \frac{((d-x)\cos(a_m) - h\sin(a_m))^2}{EI_x} dx \\ \frac{1}{k_s} &= \int_0^d \frac{1.2\cos^2(a_m)}{GA_x} dx \\ \frac{1}{k_a} &= \int_0^d \frac{\sin^2(a_m)}{EA_x} dx \end{aligned} \quad (7)$$

Where h, a_m, x, dx and d are defined in Fig. 4, E, G, A_x are Young's modulus, shear modulus and the

150 tooth section area at meshing point.

151 2.23 Function of contact stiffness

152 The stiffness of a single tooth is calculated through the aforementioned equations. However, the gear-
153 rack contact is not comprised of a single tooth, and the process of gear-rack meshing transmission involves
154 at least a pair of teeth. Therefore, it is necessary to consider the contact stiffness of a pair of teeth. In this
155 study, to simulate nonlinear Hertz contact, Hamilton's approximate Hertz contact is employed to represent
156 the contact stiffness of a single pair of meshes[15], as depicted in Equation (8):

$$157 \quad k_H = \frac{\pi L}{[4 + \pi]} \left[\left(\frac{E_1}{1 - \nu_1^2} \right) + \left(\frac{E_2}{1 - \nu_2^2} \right) \right] \quad (8)$$

158 Where ν_i ($i=1,2$) is the Poisson's ratio of gear and rack respectively.

159 2.14 Function of fillet-foundation stiffness

160 The fillet-foundation stiffness plays a crucial role in the calculation of TVMS, as the influence of gear
161 body deflection is considered. It is important to include the fillet-foundation stiffness in the TVMS
162 calculation. Sainot's fillet-foundation stiffness theory[16], as presented in Equation (9), is utilized in this
163 study. The fillet-foundation stiffness is determined by the ratio of the radius of the tooth root circle to the
164 center hole and the angle between the center line of the tooth and the joint of the tooth root circle.

$$165 \quad y_f = \frac{\cos^2 \beta}{EL} \left\{ L^* \left(\frac{u_f}{S_f} \right)^2 + M^* \left(\frac{u_f}{S_f} \right) + P^* (1 + Q^* \tan^2 \beta) \right\} \quad (9)$$

166 Where u_f , S_f , L^* , M^* , P^* 和 Q^* Cited in the literature[9].

167 2.3 white shark optimizer

168 The White Shark Optimizer (WSO) is proposed by Malik Braik[17], drawing inspiration from the
169 hunting strategies of white sharks, one of the most perilous predators of the oceans. The group-based WSO

170 algorithm is modeled after the sharks' innate hunting abilities, which rely on their superior sense of hearing,
 171 smell, and prey orientation. Due to the ever-changing positioning of the biological traits of white sharks,
 172 the WSO exhibits exceptional efficiency in avoiding local optima and accelerating the attainment of the
 173 global optimum solution for complex objective functions, as shown in Figure 5.

174 In the initial phase, the WSO algorithm begins with the white shark moving towards the optimal prey
 175 position based on its natural hunting behavior, while the initial position of the white shark is randomly
 176 generated. During the search iteration process, the vector method is utilized to explore the solution space,
 177 as presented in Equation (10):

$$178 \quad w_j^i = l_j + r \times (u_j - l_j) \quad (10)$$

179 Where w_j^i represents the vector of the i white shark on the J dimension, u_j and l_j represent the
 180 lower and upper bounds of the white shark on the J dimension respectively, and r is a random number
 181 created in the interval $[0,1]$.

182 The auditory, visual and olfactory senses are used by white sharks to search for prey. Based on this
 183 perception, the white shark moves towards its prey in a wave-like motion. By comparing the optimal prey
 184 with the known prey location, the white shark can adjust its speed during the pursuit, as presented in
 185 Equation (11).

$$186 \quad v_{k+1}^i = \mu \left[v_k^i + p_1 (w_{\text{gbest}_k} - w_k^i) \times c_1 + p_2 (w_{\text{best}_k}^{v^i} - w_k^i) \times c_2 \right] \quad (11)$$

187 v_{k+1}^i , v_k^i represents the speed at which the white shark moves to the new prey, w_{gbest_k} is the optimal
 188 prey in the current k iterations, w_k^i is position vector of the white shark i in the K step, and c_1 and c_2 are
 189 two random numbers uniformly generated within the range of $[0,1]$.

190 2.4 Multi-gear dynamics model

191 The gear meshing process is assumed to be uniform, and torsional deformation at the gearing shaft is
 192 neglected. Figure 6 illustrates gears in various meshing positions. Based on Newton's second law, combined
 193 with the time-varying meshing stiffness in Section 2, the multi-rack and gear dynamic model is developed.
 194 This model is represented by Equation (12):

$$\left\{ \begin{array}{l}
 m_i \ddot{x}_i + c_{i(t)} \dot{x}_i + k_{i(t)} x_i = F_i R_i \\
 \sum_{i=1}^8 F_i \cos \alpha = F_{load} + Ma \\
 F_1 l_1 + F_2 l_2 + F_3 l_3 + \dots + F_8 l_8 = 0 \\
 \sum_{i=1}^8 F_i = \sum_{i=1}^8 (k_i \delta_i + c_i \dot{\delta}_i) = \sum_{i=1}^8 [k_i (r\theta - e_i) + c_i (r\dot{\theta} - \dot{e}_i)]
 \end{array} \right. \quad (12)$$

196 Where: M is the total mass of the lifting system, F_{load} is the load of the lifting device, F_i is the meshing
 197 force of the gears ($i=1-8$), a is the acceleration of the lifting device, l_i is the distance from the gears to the
 198 center of gravity of the lifting device, m_i is the mass of the gears, R_i is the indexing circle of the gears, $k_{i(t)}$
 199 is the stiffness of the gears, which is calculated according to the subsection 2.2, and $c_{i(t)}$ is the damping of
 200 the gears. Damping, related to the stiffness, is calculated as shown in Equation (13):

$$c_{(t)} = 2\zeta \sqrt{k_{(t)} \frac{r_1^2 r_2^2 I_1 I_2}{r_1^2 I_1 + r_2^2 I_2}} \quad (13)$$

202 3 Case study

203 The GRDR has specific features, including the handling of large lifting weights (up to 250 tons) and
 204 exposure to different types of loads, creating complex working conditions. Parameters from the GRDR
 205 transmission unit, as shown in Table 1.

206 3.1 TVMS Analysis for rack and gear in GRDR

207 TVMS calculation methods include analytical method, finite element method, and hybrid method.

208 Finite element methods are applied for theoretical validation due to accuracy and efficiency[18, 19].

209 3.1.1 Finite element analysis setup

210 Based on the geometric and material parameters provided in Table 1, the gear and rack is modeled
211 using the finite element method. To enhance the calculation accuracy and efficiency, a multi-scale meshing
212 technique is employed for the gear and rack. The mesh cell type is selected as C3D8 cell, the number is
213 1334540, and the Jacobian of the generated mesh is greater than 0.7. The details of the meshing of the gear
214 and rack are illustrated in Figure 7.

215 The gear with 17 teeth rotates 21.177° in a single tooth meshing cycle. The meshing surface is
216 segmented into 21 parts and a load of 53125 N/mm is applied to the nodes (node 1 ~ node 21). Rack bottom
217 of the fixed frame is used as a constraint in the simulation.

218 3.1.2 Verification of calculation results

219 Figure 8 depicts the TVMS is calculated by the ISO standard Ishikawa method, the method of reference
220 [20], the method proposed in this paper, and the finite element method. Table 2 shows the results of the
221 comparison between the single tooth meshing stiffness, average meshing stiffness and obtained by the four
222 methods. Three theoretical calculations are compared with the finite element method based on the results
223 of the finite element method. The proposed method in this paper is shown to be close in the maximum
224 meshing stiffness of a single tooth and the average value of TVMS.

225 The results of bending stiffness, axial compression stiffness and meshing stiffness of single tooth
226 calculated by the reference [20] and propose model are compared.

227 The stiffness of the proposed model is calculated and compared to that of the reference 12, yielding a
228 consistently lower value, as illustrated in Figure 9. Although the shear stiffness law is akin to the meshing

229 stiffness of a single tooth, the difference in bending stiffness is accentuated during the meshing process.
230 Notably, this study accounts for the pressure angle at each meshing point on the gear and rack in the
231 developed model.

232 3.2 Optimization on gear mounting position

233 The global optimum for gear installation position optimization is employed as WSO algorithm. The
234 minimum multi-gear TVMS variance is optimized as a single objective. The optimal installation position
235 of the multi-gear system is searched efficiently while ensuring that the TVMS satisfies the stiffness variance
236 search. The parameters of the algorithm are set to a population size of 30, a maximum of 100 iterations,
237 and maximum wave and minimum current values of 0.75 and 0.07, respectively. The initial and secondary
238 velocities were set to 0.5 and 1.5. During the optimization process, the TVMS variance iterations are
239 monitored and visualized as shown in Figure 10. The algorithm and visualization provide valuable insights
240 into the optimization process and facilitate the identification of optimal design solutions.

241 Table 3 presents the parameters of the gear installation before and after optimization. The results
242 demonstrate that all optimization variables meet the necessary constraints, and the stiffness variance is
243 reduced by 89.64%. This significant reduction indicates that the smoothness of the transmission process is
244 greatly improved by optimizing the structural stiffness. The reduction in stiffness variance confirms the
245 effectiveness of the proposed optimization approach.

246 3.3 Verification of dynamic performance

247 The feasibility of the optimization results is verified by validating the dynamic model of the
248 transmission unit before and after the optimization of the gear installation position parameters. Dynamic
249 differential equations are used in the Lunge-Kutta method to obtain the dynamic response of the multi-

250 gear system. The dynamic behavior of the transmission unit is investigated to get a better understanding of
251 the effect of the optimized gear mounting distance parameters on the operation of the system.

252 Figure 11(a) depicts that the velocity curves of the transmission unit match, before and after the gear
253 installation position optimization. It shows that the gear position optimization design ensures the
254 performance of good synchronization of the lifting device. The amplitude fluctuation of the optimized
255 transmission unit in the start-up phase is alleviated, and the overall view of the speed fluctuation amplitude
256 is gentler.

257 Figure 11(b) shows that the optimized gear meshing forces are all smaller than the pre-optimization
258 gear meshing forces, with the most significant effect in Gear 1, which is reduced by about 6.58%. The gear
259 installation position is conducive to improving the dynamic characteristics of the transmission unit and its
260 reduction of gear force. The optimized gear installation position ensures stable movement of the
261 transmission unit and the service life of the gears is extended.

262 3.4 Stability test verification of transmission unit

263 This test is conducted under specific conditions, in which the GRDR load of 36 tons. The vibration of
264 the lifting box is observed during its downward speed, using the attitude detection of the lifting box.

265 3.4.1 Test setting

266 The sensor is fixed at the designated point, as shown in Figure 12. Non-gravitational acceleration
267 effects during rotation are considered. Smooth friction is made between the installation surface of the sensor
268 and the measuring surface of the transmission unit. The transmission unit is parallel to the carrier plane,
269 reducing the effect of errors on the measured data.

270 3.4.2 Test results analysis

271 In this test, real-time monitoring of the space attitude of the GRDR transmission unit was conducted
272 during its operation at speed is set as 0.28 m/s. To measure the system stability, the rotation angle of the
273 attitude sensor around the x and y axes is observed, and the changes in the angle of these axes were recorded.
274 These changes are graphically represented in Figure 13(a) (b), which demonstrates the fluctuations in the
275 rotation angles of the x and y axes, respectively.

276 Figure 13 depicts the angular fluctuation of the transmission unit around the x and y axes during
277 operation. With a velocity of 0.28 m/s, the maximum angular change around the x-axis is 0.1121° and the
278 maximum angular change around the y-axis is 0.0326° . These results show that the vibration response of
279 the GRDR transmission unit is small, and the feasibility of the design method proposed in this paper and
280 the stability of the system are verified.

281 4 Conclusion

282 In this paper, the optimization of gear mounting position is investigated for the vibration problem of
283 GRDR transmission unit, which the TVMS is considered to be affected by the gear installation position.
284 Combined with the gear and rack TVMS is developed and the global search of the White Shark algorithm
285 being utilized, the dynamic performance of the GRDR transmission unit is optimized. The feasibility of the
286 design methodology is verified based on the dynamic model developed and field tests. These findings have
287 important implications for future design and engineering efforts aimed at reducing vibration issues and
288 improving the performance of the GRDR transmission unit.

289 1. Based on the 8-gear-4-rack transmission unit in the GRDR, the TVMS model is developed by
290 combining the tooth profile function with the energy method. Other theoretical computational methods are
291 compared that proposed model is closer to the finite element method in maximum single tooth meshing

292 stiffness and average TVMS values.

293 2. The gear installation position is an effective measure to improve the dynamic performance of the
294 GRDR by reducing the fluctuations in the TVMS stiffness. The fluctuation of TVMS in the optimized
295 transmission unit is reduced by 89.64%. The magnitude of meshing force in gearing is reduced by 6.58%.

296 3. Combining the TVMS model with the WSO global optimal search algorithm, the optimal design
297 method considering the gear installation position is proposed. The effectiveness of the method is verified
298 by test results, which validate the feasibility of the method in applications.

299 Funding

300 This work of the paper was supported by the Major National Science and Technology Projects
301 [2016ZX05038-002-LH001] and study on Nonlinear Coupling Vibration Mechanism and Intelligent
302 Control Method of Steering Tool Combined Bearing-Rotor System [52204002].

303 Data availability

304 The authors confirm that the data supporting the findings of this study are available within the article.

305 Code availability

306 The authors confirm that the code supporting the findings of this study are available within the article.

307 Conflicts of interest

308 The authors declare that they have no known competing financial interests or personal relationships
309 that could have appeared to influence the work reported in this paper.

310 Author Contributions

311 All authors contributed to the study's conception and design. Jiangang Wang, Lei Shi performed
312 material preparation, data collection, and analysis. Jiangang Wang wrote the first draft of the manuscript,

313 and all authors commented on previous versions of the manuscript. All authors read and approved the final
314 manuscript.

315 5 Reference

316 1. Sun, Q.L., Jin, Z.W., Wang, J.G., et al. "Operation Strength Analysis of HXJ180 Offshore
317 Workover Rig Based on API Standard", *China Journal of Petroleum Machinery*, 50(11), pp. 58-65+72
318 (2022). doi: 10.16082/j.cnki.issn.1001-4578.2022.11.009. “ ”

319 2. Feng, D., Kang, B.W., Shi, L., et al. "Analysis of Contact Strength of Large Module Heavy Load
320 Rack and Pinion", *China Journal of Petroleum Machinery*, 46, pp. 14-9 (2018). doi:
321 10.3390/engproc2023038036.

322 3. Gao, K., Xu, X., Jiao, S. "Prediction and visualization analysis of drilling energy consumption
323 based on mechanism and data hybrid drive", *Energy*, 261, pp. 125227 (2022). doi:
324 10.1016/j.energy.2022.125227.

325 4. Shi, L., Wang, J.G., Luo, K., et al. "Analysis of Loading Distribution for SRB And TSRB
326 Combined Bearing", *SCIENTIA IRANICA*, 29, pp. 478-85 (2022). doi: 10.1201/9781482275148-5.

327 5. Farizhendy, M., Noorzai, E. and Golabchi, M. "Implementing the NSGA-II genetic algorithm to
328 select the optimal repair and maintenance method of jack-up drilling rigs in Iranian shipyards", *Ocean
329 Engineering*, 211, pp. 7548 (2020). doi: 10.1016/j.oceaneng.2020.107548.

330 6. Li, X.B., Liu, J., Wang, X.Z., et al. "Bending moment response of batter piles in clay under
331 spudcan-pile interaction", *Applied Ocean Research*, 138, pp. 103670 (2023). doi:
332 <https://doi.org/10.1016/j.apor.2023.103670>.

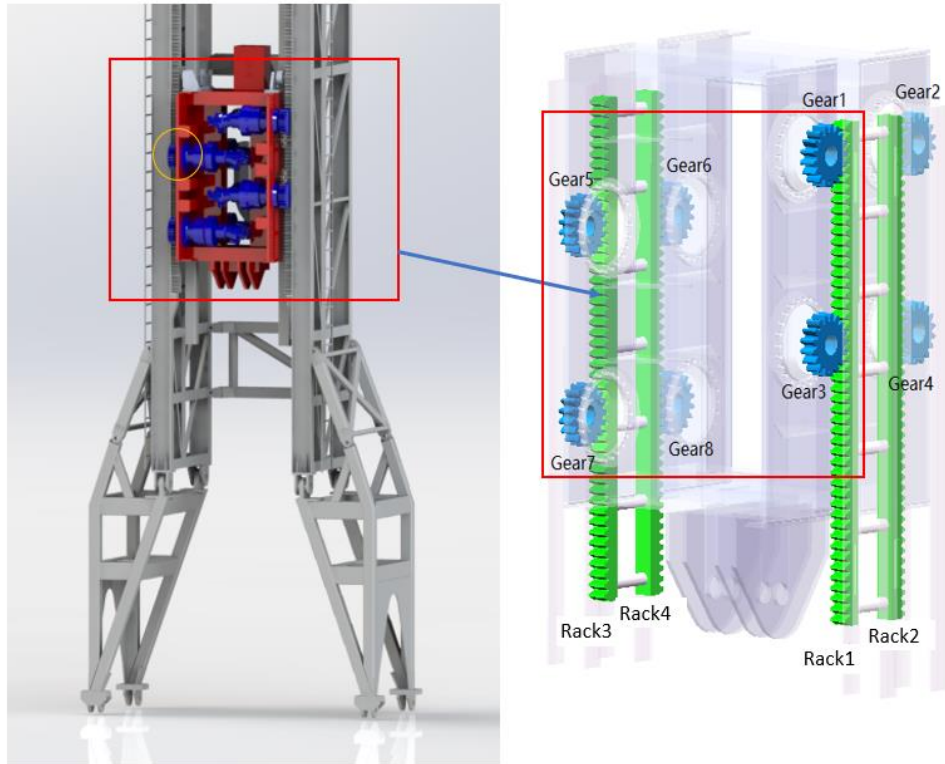
333 7. Wang, J.G., Shi, L., Feng, D., et al. "Study the muti-bolt fastening under different load positions
334 in gear rack drilling rig", *PLOS ONE*, 18, pp, e0290427(2023). doi: 10.1371/journal.pone.0290427.

335 8. Sadeghi, A.N., Arıkan, K.B., Özbek, M.E. "Modelling and controlling of drill string stick slip
336 vibrations in an oil well drilling rig", *Journal of Petroleum Science and Engineering*, 216, pp.1-11 (2022).
337 doi: 10.1016/j.petrol.2022.110759.

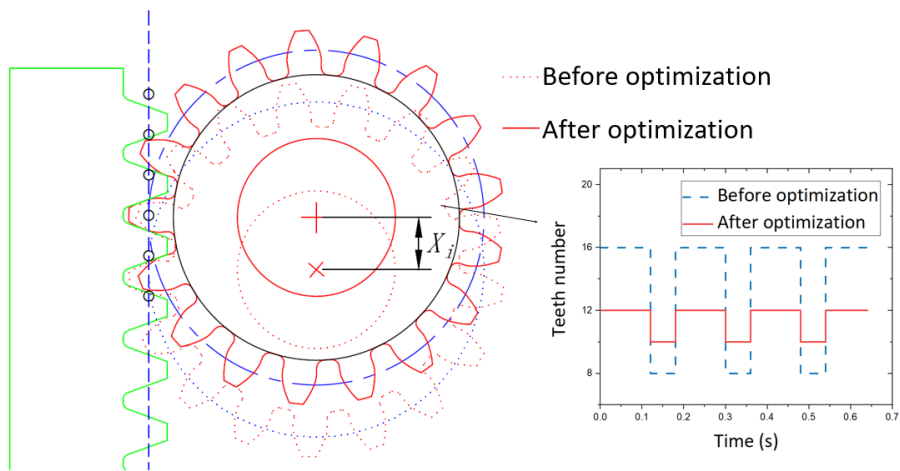
338 9. Zhang, J., Qin, X., Xie, C., et al. "Optimization design on dynamic load sharing performance for
339 an in-wheel motor speed reducer based on genetic algorithm", *Mechanism and Machine Theory*, 122, pp.

-
- 340 132-47 (2018). doi: 10.1016/j.mechmachtheory.2017.12.016.
- 341 10. C, E.B.Y.A.B., A, C.C., Jérme Bruyère b, C, E.R. and C, P. L. "Multi-objective optimization of
342 gear unit design to improve efficiency and transmission error", *Mechanism and Machine Theory*", 167, pp.
343 10499 (2022). doi: 10.1016/j.mechmachtheory.2021.104499.
- 344 11. Xu, C. "Dynamic Performance Analysis of Jack-up Platform's Jacking System with Staggering
345 Tooth", *Journal of Mechanical Engineering*, 50(19), pp.66-72 (2014). doi: 10.3901/jme.2014.19.066.
- 346 12. Mounica, D., Rao, S.S., Kumar, INN. "ANALYSIS AND OPTIMIZATION OF PINION OF A
347 JACK-UP RIG". *JETIR*, 4(10), pp. 146-155 (2017). doi: 10.1016/j.engfailanal.2020.104623.
- 348 13. Ahmed, K.S., Keng, A.K., Ghee, K.C. "Stress and stiffness analysis of a 7-teeth pinion/rack jacking
349 system of an Offshore jack-up rig", *Engineering Failure Analysis*, (2020). doi:
350 10.1016/j.engfailanal.2020.104623.
- 351 14. Lei, N., Chang, Y.L., Bian, C., et al. "Meshing Characteristic Analysis of the Gear Rack Drilling
352 Rig Hoisting System", *China Journal of Mechanical Transmission*, (2015). doi:
353 10.4028/www.scientific.net/amm.441.427.
- 354 15. Marafona, J.D.M., Marques, P.M.T., Martins, R.C., et al. "Mesh stiffness models for cylindrical
355 gears: A detailed review", *Mechanism and Machine Theory*, (2021). doi:
356 10.1016/j.mechmachtheory.2021.104472.
- 357 16. Sainsot, P., Vexex, P. and Duverger, O. "Contribution of gear body to tooth deflections—a new
358 bidimensional analytical formula", *J Mech Des*, 126(4), pp. 748-52 (2004). doi: 10.1115/1.1758252.
- 359 17. Malik, B., Abdelaziz, H., Jaffar, A., et al. "White Shark Optimizer: A novel bio-inspired meta-
360 heuristic algorithm for global optimization problems", *Knowledge-Based Systems*, 243, pp. 108457 (2022).
361 doi: 10.1016/j.knosys.2022.108457.
- 362 18. Thirumurugan R. and Gnanasekar N. "Influence of finite element model, load-sharing and load
363 distribution on crack propagation path in spur gear drive", *Engineering Failure Analysis*, 110, pp. 104383
364 (2020). doi: 10.1016/j.engfailanal.2020.104383.
- 365 19. Bejar F, Perret-Liaudet J, Bareille O, et al. "Review and benchmarking study of different gear
366 contact analysis software in terms of the static transmission error response", *Results in Engineering*", 22,
367 pp. 102286 (2024). doi: 10.1016/j.rineng.2024.102286.

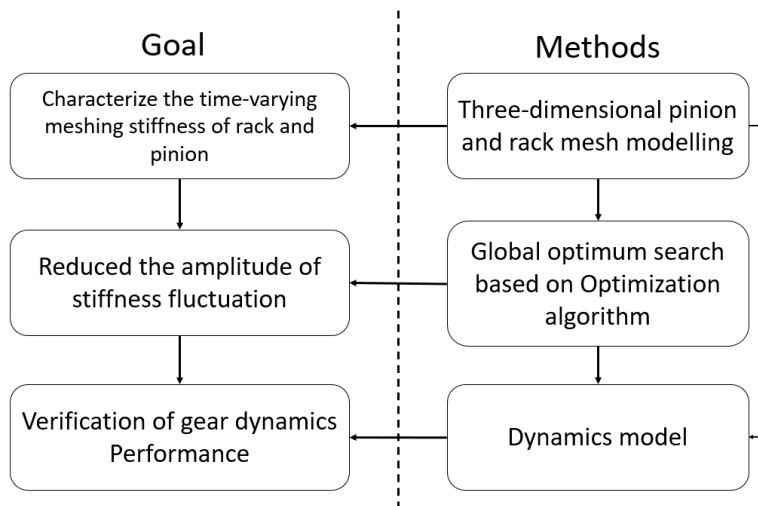
368 20. Rezaei, E., Poursina, M., Rezaei, M., et al. "A new analytical approach for crack modeling in spur
369 gears", *Jordan Journal of Mechanical and Industrial Engineering*, 13(2), pp. 69-74 (2019). doi:
370 10.4271/2021-01-0699.
371



372
373 **Fig. 1 Diagram of the gear distribution in GRDR transmission unit**



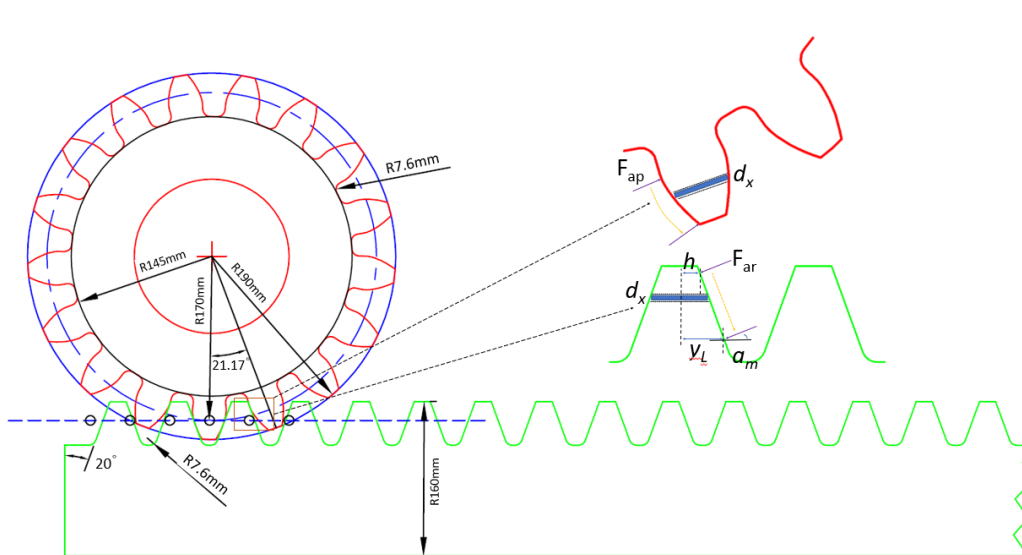
374
375 **Fig. 2 Effect of installtion position on phase difference**



376

377

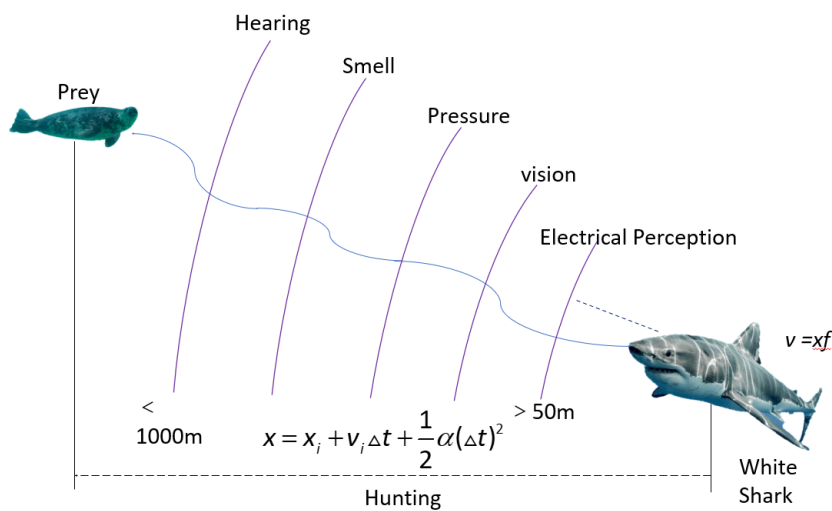
Fig. 3 Methodological framework of gear installation position design



378

379

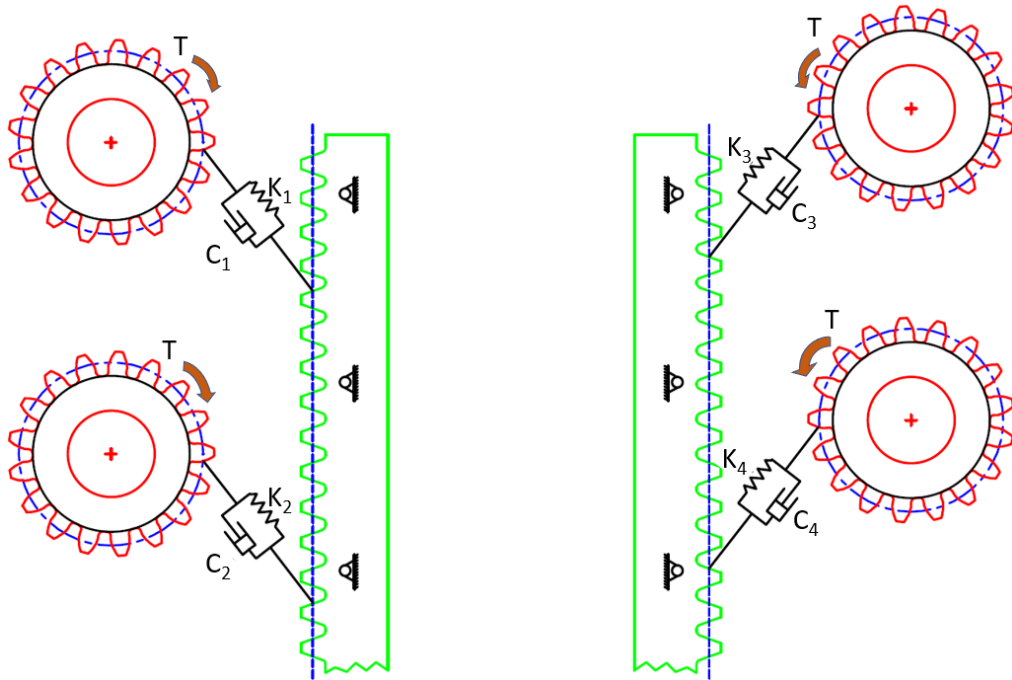
Fig. 4 Schematic of the load of tooth



380

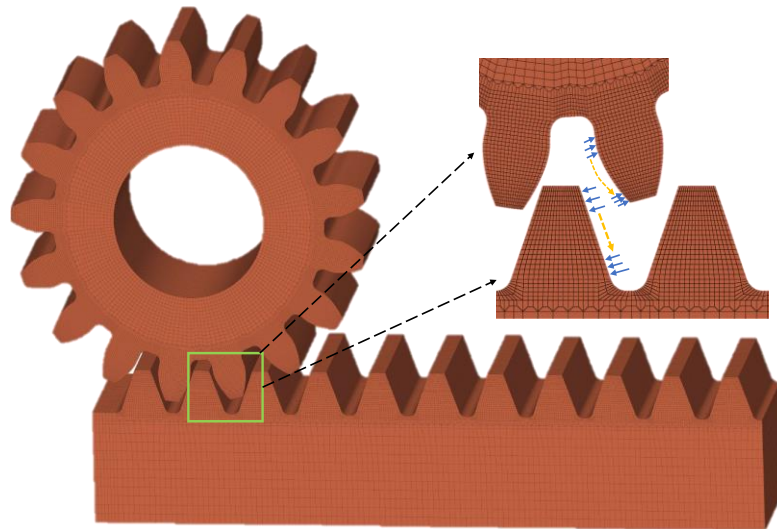
381

Fig. 5 White sharks track prey



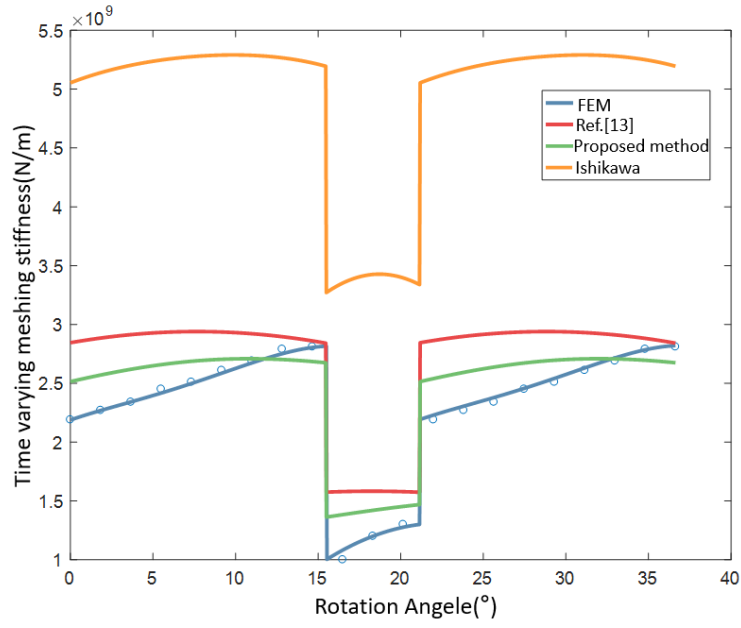
382
383

Fig. 6 Dynamics model of gear and rack



384
385

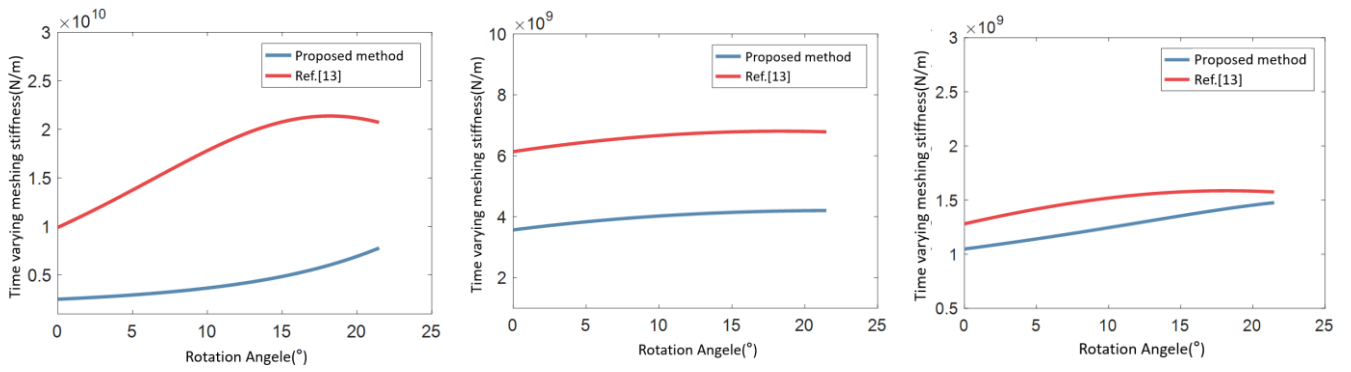
Fig. 7 Finite element model considering meshing Angle



386

387

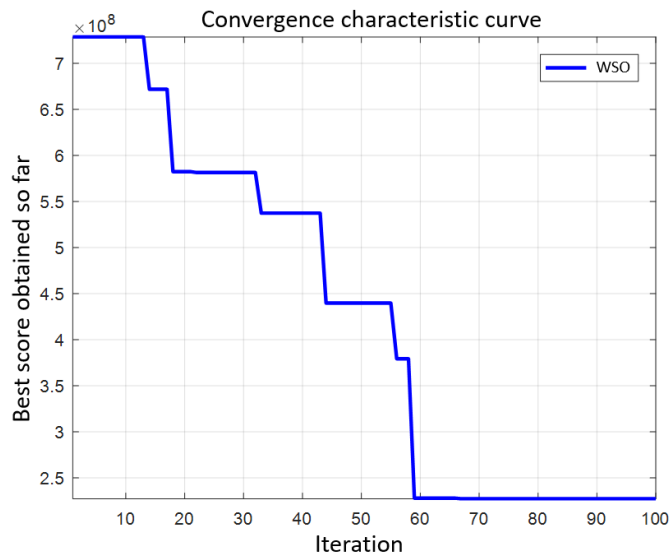
Fig. 8 TVMS based on different methods



388

389

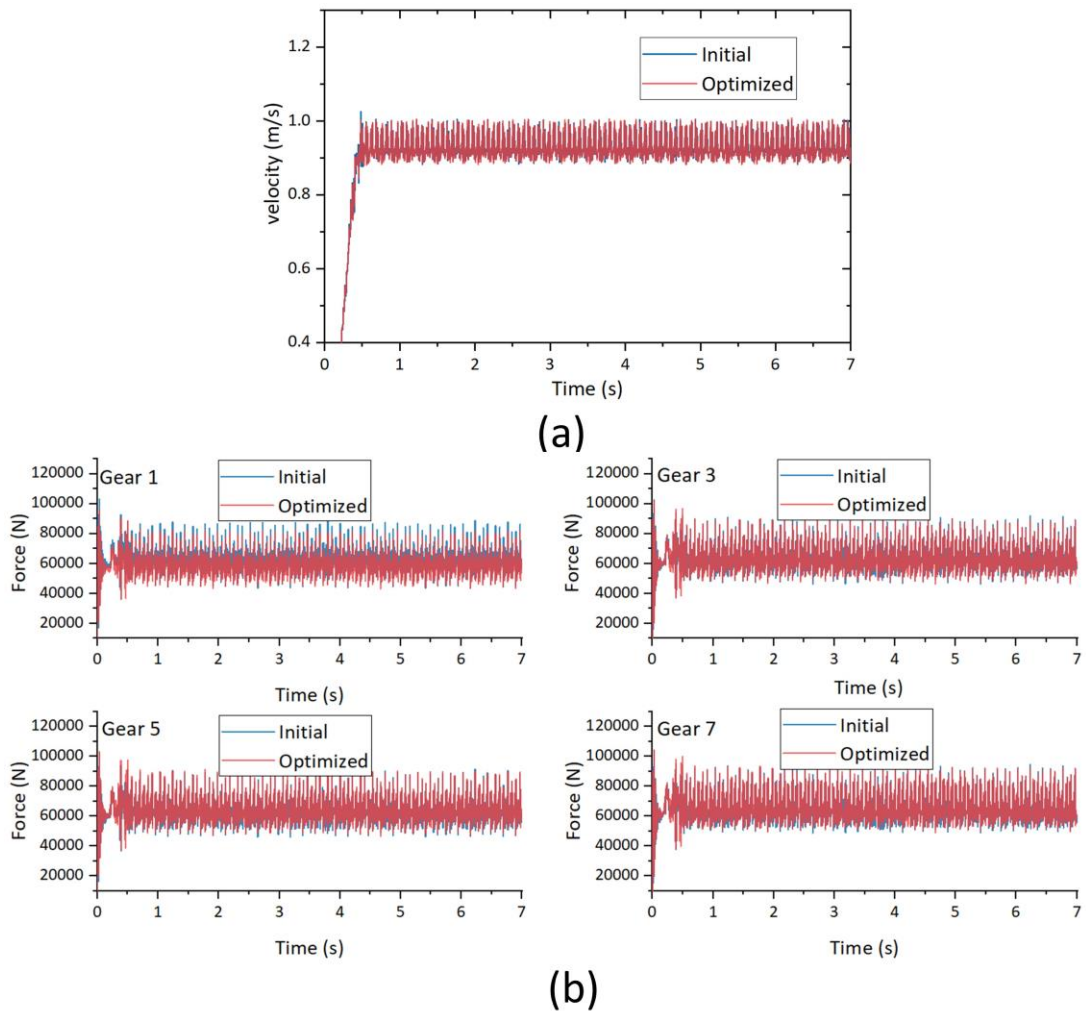
Fig. 9 Comparison of single tooth meshing stiffness curves based on different methods



390

391

Fig. 10 Convergence Curves



392

393

Fig. 11 Velocity and gear meshing force before and after optimization



Fig. 12 Orientation of attitude sensor installation

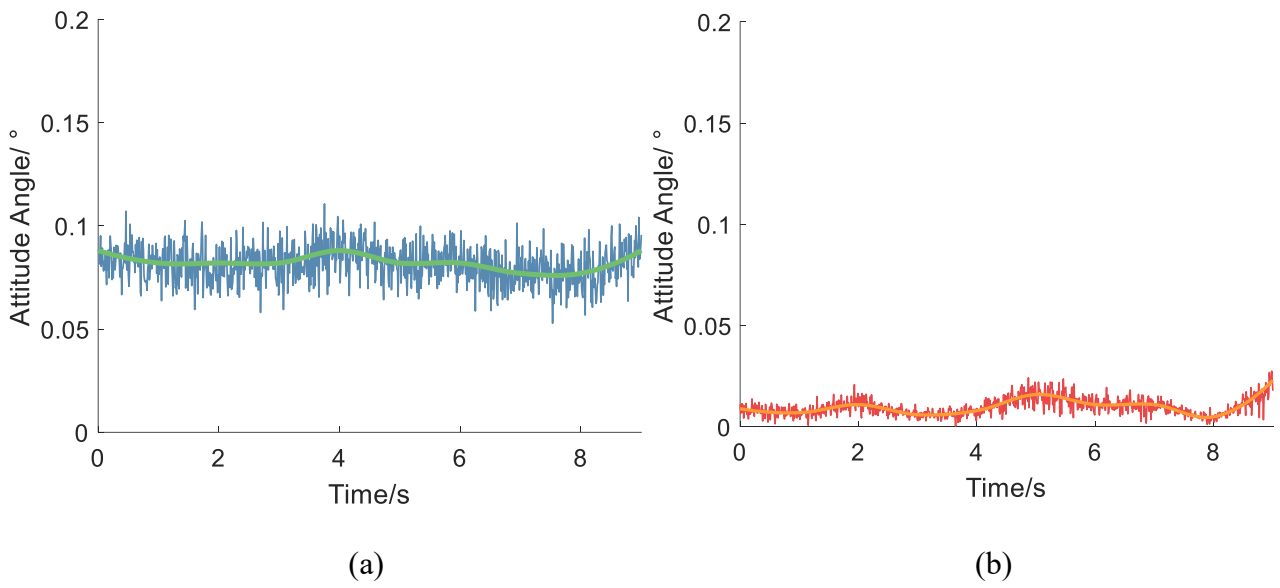


Fig. 13 x/y axis attitude angle detection in 0.28m/s velocity

404

Table 1 Parameters of gear and rack

Parameters	Value
Modulus $m(\text{mm})$	20
Pressure angle α ($^\circ$)	20
Number of teeth Z	17
Pitch diameter (mm)	340
Tooth width $L(\text{mm})$	120
Gear elastic modulus E_1 (GPa) / Poisson ratio ν_1	207 / 0.254
Rack elastic modulus E_2 (GPa) / Poisson ratio ν_2	212 / 0.28

405

406

Table 2 Comparison of TVMS calculations

Method	Maximum meshing stiffness of a single tooth (N/m)	Comparison with finite element(%)	The average value of TVMS /(N/m)	Comparison with finite element(%)
Ishikawa	3.43e+09	62	4.74E+09	51
Reference	1.58e+09	17	2.55E+09	9
Proposed	1.46e+09	10	2.33E+09	0.4
Finite element	1.30E+09	-	2.32e+09	-

407

408

Table 3 Optimize before and after parameters

	Gear 1	Gear 3	Gear 5	Gear 7	Variance of meshing stiffness
Before optimization	0	0	0	0	2.19e+09
After optimization	+10	+56	+25	+39	2.27e8

409

410

411 Biographies

412 Jiangan Wang is a current Ph.D. student at Yangtze University. As a major participant, he has
413 participated in 3 national provincial and ministerial projects and Published 8 related papers. His research

414 interests: theoretical and technical application research in the design, diagnosis and dynamic simulation of
415 petroleum machinery.

416 Lei Shi, Associate Professor, his major in oil field equipment, published several papers and participated
417 in the translation of a series of books on foreign oil and gas exploration and development progress. He has
418 participated in 6 projects at national and provincial levels published 8 first-author academic papers in
419 relevant academic journals.

420 Ding Feng is a Professor of Mechanical Engineering at Yangtze University, China. He received his
421 Ph.D. at the China University of Petroleum (Beijing). His main research areas are design, testing and
422 diagnostics of oil and gas drilling and completion tools and equipment and offshore engineering equipment
423 and tubular column mechanics and dynamic simulation technology. He has participated in nearly 90
424 projects at national and provincial levels and published 242 relevant academic papers.

425 Sun Qiaolei, Associate professor, has presided over 8 vertical and horizontal projects of Hubei Natural
426 Science Foundation, participated in more than 10 projects of National Natural Science Foundation, youth
427 projects and national major special projects, and published more than 40 relevant journal papers;.

428 Enming Miao is a professor and Ph.D. supervisor in the School of Instrument Science and
429 Optoelectronic Engineering at the Hefei University of Technology. His main research interests are precision
430 mechanical engineering, accuracy theory, thermal error compensation of CNC machine tools, and structural
431 design theory and application technology of mechanical thermal robustness. Published more than 50 papers.